

## Charge-Discharge Cycling Induced Structural and Chemical Evolution of $\text{Li}_2\text{MnO}_3$ Cathode for Li-ion Batteries

Pengfei Yan<sup>1</sup>, Jianming Zheng<sup>2</sup>, Ji-Guang Zhang<sup>2</sup>, and Chong-Min Wang<sup>1</sup>

<sup>1</sup>Environmental Molecular Sciences Laboratory, Pacific Northwest National Laboratory, 902 Battelle Boulevard, Richland, WA 99352, USA

<sup>2</sup>Energy and Environmental Directorate, Pacific Northwest National Laboratory, 902 Battelle Boulevard, Richland, WA 99352, USA

Capacity and voltage fading of lithium-and-manganese-rich (LMR) cathodes is a major challenge for the application of this category of material, which is believed to be associated with the structural and chemical evolution of the materials.[1-3] As one of the most promising cathode materials for next generation lithium ion batteries, LMR cathode materials have the expression  $x\text{LiMO}_2 \cdot (1-x)[\text{Li}_2\text{MnO}_3]$  ( $M=\text{Mn, Ni, Co, } 0 \leq x < 1$ ). As the parent component of LMR,  $\text{Li}_2\text{MnO}_3$  cathode materials also attracted much attention for many reasons. First,  $\text{Li}_2\text{MnO}_3$  itself has a very high theoretical capacity. Second, it can enhance our fundamental understanding of the electrochemistry of  $\text{Mn}^{4+}$ -containing cathode materials. Thirdly, we can obtain the knowledge necessary for design new LMR cathode materials.  $\text{Li}_2\text{MnO}_3$  cathode was initially believed electrochemically inert because all the Mn cations are  $\text{Mn}^{4+}$  in this material until Kalyani et al. demonstrated that  $\text{Li}_2\text{MnO}_3$  could be electrochemically activated in 1999.[4] It has been claimed that prolonged cycling could transform  $\text{Li}_2\text{MnO}_3$  to  $\text{LiMn}_2\text{O}_4$ -spinel.[5, 6] However, recently X-ray absorption spectroscopy results from cycled sample are not consistent with the  $\text{LiMn}_2\text{O}_4$ -spinel structure, instead the P3 structure was proposed.[7] In a chemically delithiated  $\text{Li}_2\text{MnO}_3$  sample, Wang et al. observed the formation of  $\text{MnO}_2$  phase.[8] Up to now, it is still not clear which structure is formed after charge-discharge cycles and how the structure evolves during the cycling of  $\text{Li}_2\text{MnO}_3$  cathode.

In this work, we report the detailed structural and chemical evolutions of  $\text{Li}_2\text{MnO}_3$  cathode captured by using aberration corrected scanning/transmission electron microscope (S/TEM) after certain numbers of charge-discharge cycling of the batteries. It is found that structural degradation occurs from the very first cycle and is spatially initiated from the surface of the particle and propagates towards the inner bulk as cyclic number increase, featuring the formation of the surface phase transformation layer and gradual thickening of this layer. The structure degradation is found to follow a sequential phase transformation: monoclinic  $C2/m \rightarrow$  tetragonal  $I41 \rightarrow$  cubic spinel (as shown in Figure 1), which is consistently supported by the decreasing lattice formation energy based on DFT calculations. For the first time, high spatial resolution quantitative chemical analysis reveals that 20% oxygen in the surface phase transformation layer is removed and such newly developed surface layer is a Li-depleted layer with reduced Mn cations (Figure 2). This work demonstrates a direct correlation between structural degradation and cell's electrochemical degradation. In a more general term, since  $\text{Li}_2\text{MnO}_3$  cathode is the parent compound for LMR cathode, this work will enhance our understanding on the degradation mechanism of LMR cathode materials during cycling.

### References:

- [1] F. Lin, I. M. Markus, D. Nordlund, T. C. Weng, M. D. Asta, H. L. Xin, M. M. Doeff, *Nature Commun.* **5** (2014), 3529.

- [2] M. Gu, I. Belharouak, J. Zheng, H. Wu, J. Xiao, A. Genc, K. Amine, S. Thevuthasan, D. R. Baer, J.-G. Zhang, N. D. Browning, J. Liu, C. Wang, *ACS Nano* **7** (2012), 760.
- [3] P. Yan, A. Nie, J. Zheng, Y. Zhou, D. Lu, X. Zhang, R. Xu, I. Belharouak, X. Zu, J. Xiao, K. Amine, J. Liu, F. Gao, R. Shahbazian-Yassar, J. G. Zhang, C. M. Wang, *Nano Lett.* **15** (2015), 514.
- [4] P. Kalyani, S. Chitra, T. Mohan, S. Gopukumar, *J. Power Sources* **80** (1999), 103.
- [5] A. D. Robertson, P. G. Bruce, *Chem. Mater.* **15** (2003), 1984.
- [6] J. Reed, G. Ceder, A. Van der Ven, *Electrochem. Solid-State Lett.* **4** (2001), A78.
- [7] J. Rana, M. Stan, R. Kloepsch, J. Li, G. Schumacher, E. Welter, I. Zizak, J. Banhart, M. Winter, *Adv. Energy Mater.* **4** (2014), 1300998.
- [8] R. Wang, X. Q. He, L. H. He, F. W. Wang, R. J. Xiao, L. Gu, H. Li, L. Q. Chen, *Adv. Energy Mater.* **3** (2013), 1358.

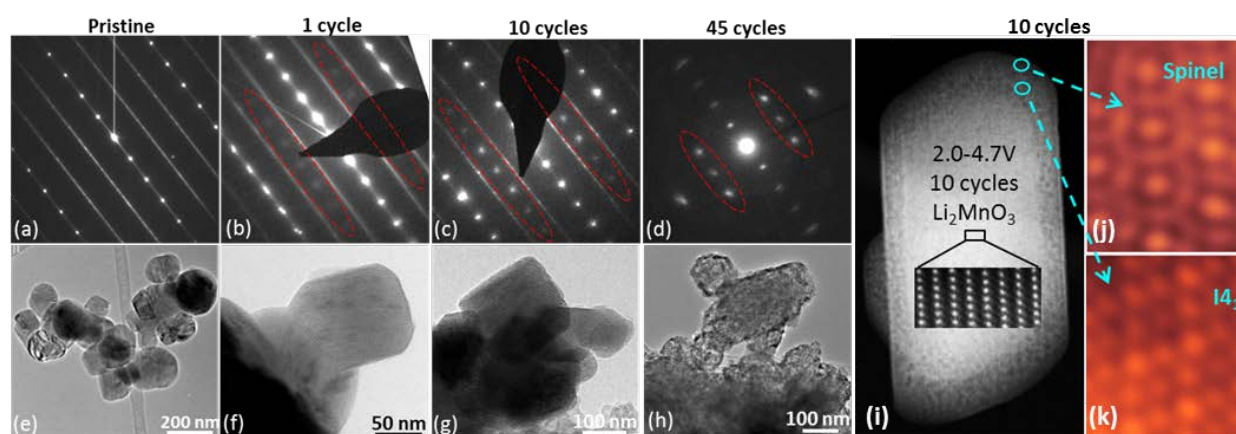


**Figure 1.** (a-d) [100]m zone SAED patterns from different samples. Red arrows in (a) highlight the streaks due to the formation of stacking faults and lamellar domains in  $C2/m$  structure. Dashed red circles in (b-d) highlight extra diffraction spots due to structure transformation from  $C2/m$  to spinel. (e-h) TEM images to show particle morphology evolution from pristine sample to 45-cycles sample. (i-k) STEM-HAADF images show lattice structure change after 10 cycles.

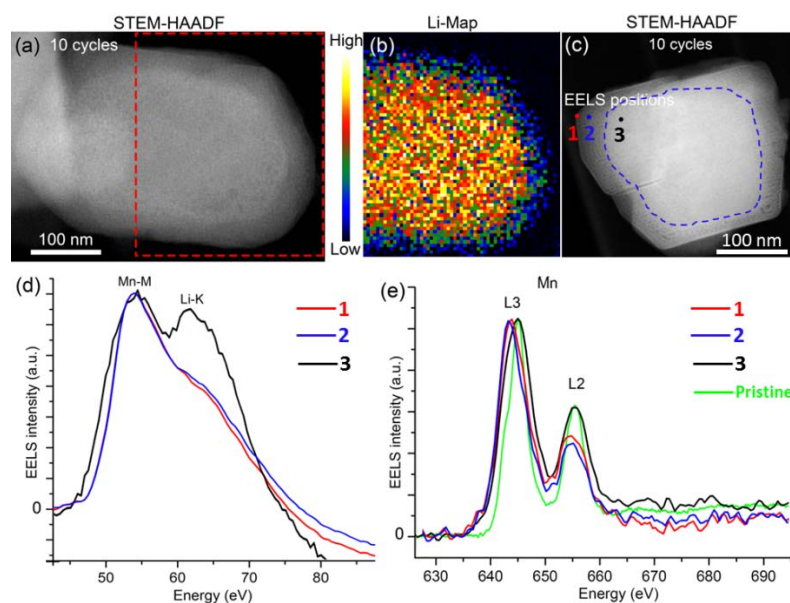


**Figure 2.** (a, b) STEM-EELS mapping of a 10-cycles sample. The mapping area is highlighted by dashed red frame in (a). (c-e) STEM-EELS analysis of 3 positions (1, 2 and 3, shown in (c)) of a 10-cycles sample. The spectra are normalized using Mn-M edge and Mn-L3 edge in (d) and (e), respectively. In (d), the depressed Li-K edge in positions 1 and 2 indicates less Li content at the two positions. In (e), the depressed Mn-L2 edge was shown for the 10-cycles sample as compared with pristine sample.